SANDIA REPORT
SAND2008-2638
Unlimited Release
Printed May 2008

Oxidation of Zirconium Alloys in 2.5 kPa Water Vapor for Tritium Readiness

Bernice E. Mills

Prepared by
Sandia National Laboratories
Albuquerque, New Mexico 87185 and Livermore, California 94550

Sandia is a multiprogram laboratory operated by Sandia Corporation,
a Lockheed Martin Company, for the United States Department of Energy's
National Nuclear Security Administration under Contract DE-AC04-94AL85000.

Issued by Sandia National Laboratories, operated for the United States Department of Energy by Sandia Corporation.

Available to DOE and DOE contractors from
U.S. Department of Energy
Office of Scientific and Technical Information
P.O. Box 62
Oak Ridge, TN 37831

Telephone: (865) 576-8401
Facsimile: (865) 576-5728
E-Mail: reports@adonis.osti.gov
Online ordering: http://www.osti.gov/bridge

Available to the public from
U.S. Department of Commerce
National Technical Information Service
5285 Port Royal Rd.
Springfield, VA 22161

Telephone: (800) 553-6847
Facsimile: (703) 605-6900
E-Mail: orders@ntis.fedworld.gov
Online order: http://www.ntis.gov/help/ordermethods.asp?loc=7-4-0#online

SAND2008-2638
Unlimited Release
Printed November 2007

Oxidation of Zirconium Alloys in 2.5 kPa Water Vapor for Tritium Readiness

Bernice E. Mills
Materials Chemistry Department
Sandia National Laboratories
P. O. Box 969
Livermore, California 94550

ABSTRACT

A more reactive liner material is needed for use as liner and cruciform material in tritium producing burnable absorber rods (TPBAR) in commercial light water nuclear reactors (CLWR). The function of these components is to convert any water that is released from the Li-6 enriched lithium aluminate breeder material to oxide and hydrogen that can be gettered, thus minimizing the permeation of tritium into the reactor coolant. Fourteen zirconium alloys were exposed to 2.5 kPa water vapor in a helium stream at 300°C over a period of up to 35 days. Experimental alloys with aluminum, yttrium, vanadium, titanium, and scandium, some of which also included ternaries with nickel, were included along with a high nitrogen impurity alloy and the commercial alloy Zircaloy-2. They displayed a reactivity range of almost 500, with Zircaloy-2 being the least reactive.

This page intentionally left blank.

ACKNOWLEDGMENT

The group at PNNL, of whom David Senor is the contact for this work, is gratefully acknowledged for supplying samples for this work. Josh Whaley's assistance in setting up and servicing the equipment, both flow and data collection, was invaluable.

This page intentionally left blank.

TABLE OF CONTENTS

This page intentionally left blank.

Oxidation of Zirconium Alloys in 2.5 kPa Water Vapor for Tritium Readiness

INTRODUCTION

Currently the zirconium alloy Zircaloy-4 (nominally 0.1 wt. % Cr, 0.1 wt. % Fe, 0.05 wt. % Ni, 0.12 wt. % O, 1.4 wt. % Sn, 98.5 wt. % Zr) is used as a liner material in tritium producing burnable absorber rods (TPBARs) used to breed tritium in commercial light water nuclear reactors (CLWRs). Liners serve to convert the fraction of tritium released from the ^{6}Li enriched lithium aluminate high-temperature ceramic pellets in the form of tritiated water to oxide and molecular tritium (T_2), which can then be removed by a nickel-plated Zircaloy getter along with the tritium released from the pellets as T_2. It is necessary to remove all of the T_2O and T_2 produced to minimize the source for diffusion of tritium through the TPBAR cladding into the reactor cooling water.

A TPBAR is composed of 12 pencils, each with a liner about 12 inches long. The pencils each currently contain a stack of two inch pellets of lithium aluminate. Where the pencils abut there is a pencil-pencil gap and between the pellets there are pellet-pellet interfaces. Assemblies are made of 24 rods, a number of which are placed in a reactor in place of conventional burnable absorber rods, which absorb the excess neutrons at the beginning of the fuel cycle. [Figure 1] As the number of rods deployed has increased with more recent experimental cycles, an excess of tritium above that predicted has been observed in the cooling water, indicating that our understanding of the processes occurring in the TPBARs is not complete. More data on the behavior of the materials in the TPBAR is needed. Sandia has re-instituted a modeling effort that was used several years ago to produce an early design for TPBARs, but only recently have the tools to gather data to benchmark these models to the performance of the liner materials become available.

Recent advances in diagnostics for examining the oxide thickness on the surface of the liner material has allowed, for the first time, the entire 12 foot length of the liner to be mapped during Cycle 6 post-irradiation examination. It is clear from these results that there are some areas of the TPBAR where the liner is not functioning well enough to preclude water getting out of the center of the TPBAR and contacting the cladding. A full length getter is being developed which will prevent transport of water between pencil-pencil gaps directly to the cladding. However, a more reactive alloy of zirconium is needed to decompose all of the water before it can be transported to the ends of the cladding or to either of the end plugs.

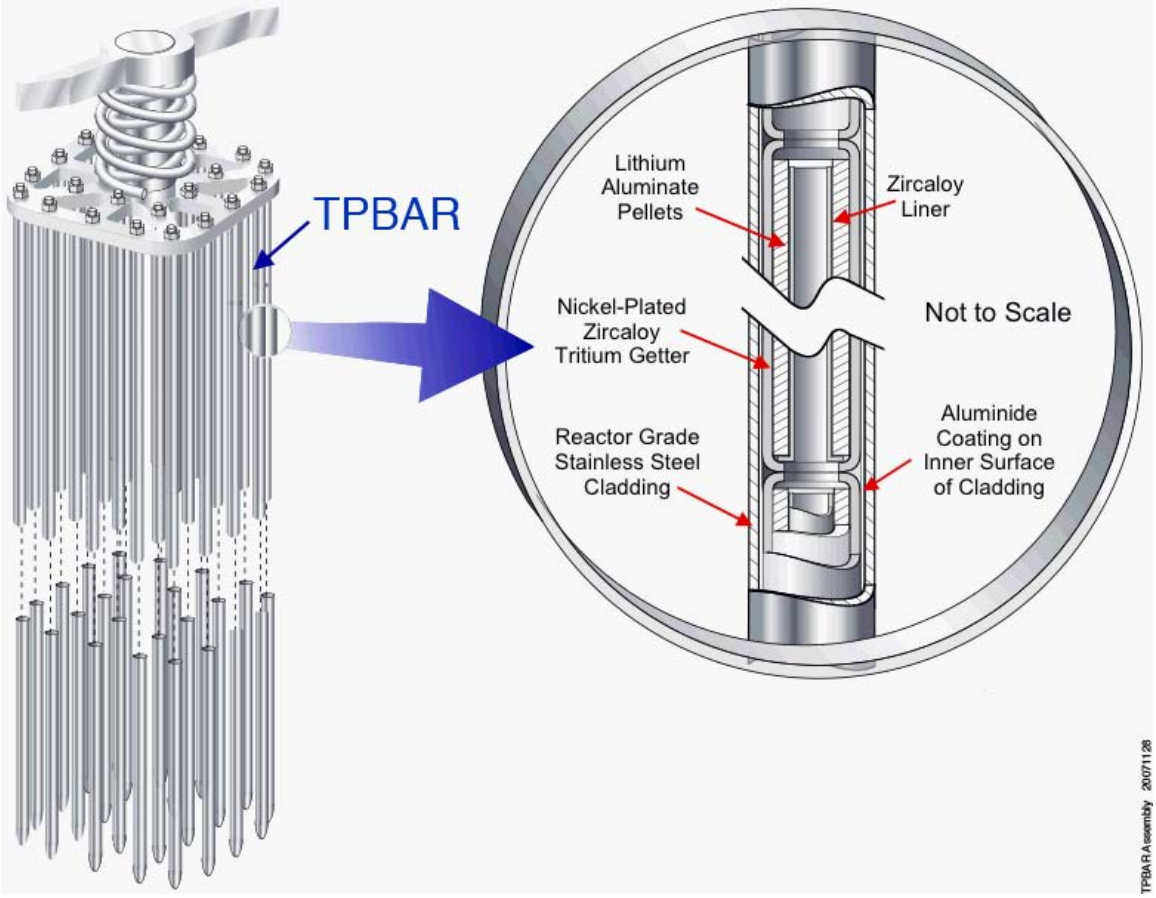

Figure 1. Diagram of assembly of TPBARs and cross-sectional diagram of the area around a pencil-pencil interface [Denton].

Zirconium alloys are commonly used as getters [Schemel]. Over the years there have been many good review articles on the oxidation of zirconium and its alloys in both water and oxygen and both in and out of a radiation field [Thomas, Cox, Douglass, Causey]. Zirconium, with a very low-cross section for absorption of thermal neutrons of 0.18 barns [Parfenov], is an excellent candidate for use in nuclear reactors as fuel cladding (for ~3 years) and for structural members (for up to 30 years) if it can withstand oxidation [Cox]. Zirconium forms a protective self-healing oxide surface film which is very resistant to most corrosive media except halides in an oxidizing atmosphere. Like aluminum and titanium, the oxide film regenerates itself in most environments when mechanically damaged. However, the zirconium oxide film is much more corrosion resistant [Yau, 1989].

Zirconia and doped zirconias have also been extensively studied as the nature of the oxidized layer is important to the corrosion behavior of the metal. In oxygen corrosion of zirconium, the outer portion of the oxide supports diffusion of interstitial anions. The zone next to the metal is dominated by the diffusion of oxygen vacancies as the oxide changes from *p*-type to *n*-type with the decrease of the oxygen partial pressure from that at the oxide surface to the equilibrium dissociation pressure of the oxide, on the order of 10^{-30} to 10^{-50} atm. Alloying additions from

valences other than zirconium's 4 will therefore have opposing effects on the different zones of the oxide, confounding prediction of corrosion rate trends [Nasrallah]. In the same group as zirconium, titanium can have 3 as well as the preferred 4 valence and is known to increase corrosion of zirconium. In group IVB, carbon, silicon, tin, and lead, each of which can assume a lower valence, have been shown to increase Zr corrosion. This may seem strange because Sn is an important alloying addition in the Zircaloys. In those cases the tin is working to counteract the effects of nitrogen impurity and in concert with other alloying additions such as iron, nickel, and chromium to produce a more corrosion resistant alloy [Thomas]. These alloys do not have the corrosion resistance of pure zirconium, but have greater yield strength and a more predictable corrosion rate [Knittel, 1983]. Antimony also can counteract the effects of nitrogen, but much less effectively than Sn [Thomas].

Additional elements known to have harmful effects on corrosion are: nitrogen, sodium, magnesium, aluminum, chlorine, calcium, scandium, vanadium, manganese, zinc, gallium, yttrium, niobium, cadmium, lanthanum, cerium, thorium, and uranium [Thomas]. Nitrogen, aluminum, and titanium impurities are known to affect corrosion resistance by causing a rapid transition from the typical initial period of decreasing corrosion to a more rapid linear corrosion rate. Nitrogen does this at as little as 40 ppm [Craig].

Zirconium oxidation has been shown to be accelerated by surface contamination with acetates of copper, lithium, calcium, and cobalt. This initial rate increase is followed by lower corrosion rates as the corrosion progresses. Although Thomas reports that copper is innocuous at the usual impurity level, Cu has been identified in surface contamination from annealing in silica capsules that causes accelerated oxidation. Surface contamination with vanadium has also been shown to accelerate film growth [Demant]. Lithium is an unacceptable alloying addition because it transmutes to tritium and helium. Cobalt makes the notorious Co-60.

Any new alloys developed must be able to be fabricated, first into sheet for testing, and ultimately into tubing for use as liners in in-reactor tests [Johnson] and then in TPBARs. Zirconium is only miscible with titanium, hafnium, and scandium (all near neighbors in the periodic table). Hf, which is below Zr in group IVA, is found in nature with Zr and, because of its high neutron cross section (105 barns, compared with 0.18 for Zr), must be removed for use in a nuclear reactor [Parfenov]. Most other elements form intermetallic compounds with zirconium as they have very low solubility [Yau, 2005]. Some alloying additions must be excluded because of high neutron cross section and some because they form low melting phases which make the alloy difficult to process. Fortunately it is not necessary to weld the tubing used for liners in the TPBARs, but a new design that has been suggested to remove water from the ends of the TPBARs does include an autologous weld so that due consideration must be taken of the incorporation of impurities that can effect corrosion during welding of this very reactive material. Zircaloy-2 has been shown to have no apparent irradiation effect on corrosion rate [Kass]. Such experiments are beyond the scope of this work, but a follow-on in-reactor test with successful candidates is planned.

EXPERIMENTAL

Zirconium alloys were fabricated at ATI Wah Chang in approximately 200 g melts and rolled into a sheet. The composition of the alloys fabricated is listed in Table 1. Two sets of coupons were cut from the sheet by electro-discharge machining (EDM) with a brass (an alloy of copper and zinc) wire. 40 x 17 mm samples were used for mass gain measurements and returned to test after measurement. One coupon of 5 x 8 mm samples of each alloy composition was removed at each point where a mass measurement was taken. The sheet was not rolled as thin as the liner, but the masses of coupons cut from the sheet were well in the range of the balance that was used to measure oxidation. Each alloy composition was identified by a letter and each sample was marked with a unique letter/number code.

Table 1. Identifiers, nominal compositions, and compositional analysis of each of the alloys.

	A	**B**	**C**	**D**	**E**	**H**	**J**	**K**	**L**	**M**	**R**	**S**	**T**	**V**	
	1.5 Y	1.0 Al	5.0 V	1.0 Ti	1.0Al 0.5Ni	2Ti 0.5Ni	5V 0.1Ni	5V 0.7Ni	1.5Y 0.5Ni	ZR-2	>200 ppm I	0.1 Sc	2Ti 0.5Ni	0.5Sc 0.1Ni	
Lot #	TTP 1	TTP 2	TTP 4	TTP 5	TTP 7	TTP 8 A	TTP 9	TTP 10	TTP 11	TTP 13	TTP 3	TTP 6	TTP 8 B	TTP 12	Lot #
Al	<.01	**0.95**	<.01	<.01	**0.97**	<.01	<.01	<.01	<.01	75	0.01	0.01	<.01	<.01	Al
B	0.25	<.25	0.25	0.25	0.25	0.25	0.25	<.25	0.25	<.25	<.25	<.25	<.25	<.25	B
C	41	51	52	47	64	60	48	142	58	180	54	37	44	35	C
Ca	0.01	0.01	0.01	0.01	0.01	0.01	0.01	0.01	0.01	<10	<25	<25	<25	<25	Ca
Cd	<1	<1	<1	<1	<1	<1	<1	<1	<1	<.25	<.25	<.25	<.25	<.25	Cd
Co	<10	<10	<10	<10	22	25	<10	32	22	<10	<10	<10	<10	<10	Co
Cr	<.01	<.01	<.01	<.01	<.01	<.01	<.01	<.01	<.01	980	<50	<50	<50	<50	Cr
Cu	<25	<25	<25	<25	<25	29	<25	<25	<25	<25	<25	<25	26	<25	Cu
Fe	<.01	<.01	<.01	<.01	<.01	<.01	<.01	<.01	<.01	1390	210	180	210	180	Fe
H	24	35	16	13	35	40	18	25	34	20	21	17	15	23	H
Hf	62	60	60	59	59	60	59	59	59	100	51	51	51	51	Hf
Mg	<.01	<.01	<.01	<.01	<.01	<.01	<.01	<.01	<.01	<10	<25	<25	<25	<25	Mg
Mn	<25	<25	<25	<25	<25	<25	<25	<25	<25	<25	<25	<25	<25	<25	Mn
Mo	<10	<10	20	<10	<10	<10	19	20	<10	<10	<10	<10	<10	<10	Mo
N	<20	<20	<20	<20	<20	<20	<20	<20	<20	39	**280**	<20	<20	21	N
Nb	<50	<50	<50	<50	<50	<50	<50	<50	<50	<50	<50	<50	<50	<50	Nb
Ni	<.01	<.01	<.01	<.01	**0.47**	**0.52**	**0.099**	**0.65**	**0.53**	490	<.01	<.01	**0.55**	**0.1**	Ni
O	400	400	410	400	440	590	440	450	480	1420	510	370	410	380	O
P	4	<3	<3	<3	<3	<3	<3	<3	<3	5	6	4	<3	4	P
Sc	<.01	<.01	<.01	<.01	<.01	<.01	<.01	<.01	<.01		<.01	**0.093**	<.01	**0.45**	Sc
Si	<.01	<.01	<.01	<.01	<.01	<.01	<.01	<.01	<.01	83	<10	<10	<10	<10	Si
Sn	<35	<35	<35	<35	<35	<35	<35	<35	<35	1.44	<35	<35	<35	<35	Sn
Ti	<.01	<.01	<.01	**0.99**	<.01	**2.02**	<.01	<.01	<.01	<25	<.01	<.01	**2**	<.01	Ti
U	<1.0	<1.0	<1.0	<1.0	<1.0	<1.0	<1.0	<1.0	<1.0	<1.0	<1.0	<1.0	<1.0	<.10	U
V	<.01	<.01	**4.83**	<.01	<.01	<.01	**4.7**	**4.8**	<.01	<25	<.01	<.01	<.01	<.01	V
W	<30	<30	<30	<30	<30	<30	<30	<30	<30	<30	<30	<30	<30	<30	W
Y	**1.53**	<.01	<.01	<.01	<.01	<.01	<.01	<.01	**1.35**		<.01	<.01	<.01	<.01	Y
ID	M-12971	M-12972	M-12973	M-12974	M-12975	M-12976	M-12977	M-12978	M-12979	M-13031	M-12990	M-12991	M-12992	M-12993	ID

A 7 foot long 50 mm O.D. 46 mm I.D. quartz tube with -torr o-ring sealed compression fittings end caps was used to contain the helium/water atmosphere for the corrosion experiments. Three 4 foot long 20.5 mm O.D. 18 mm I.D. quartz tubes were used to contain the samples. The tubes were placed in a four foot long Linberg MoldaTherm® model 55667 hinged tube furnace with three 1 foot heating zones. The zones were each independently controlled by a thermocouple built into the furnace and the controllers could be set in increments of 1 K. The temperature could be controlled to within 1 K over an 18 inch section as measured with a thermocouple that

was slowly moved inside one of the tubes, waiting at each point for the temperature to stabilize (Figure 2). The temperature in the furnace was monitored during heat-up with a thermocouple placed in the center of the tubes and the temperature ramped up slowly to avoid overshooting the target temperature. As the clam-shell furnace could be opened, terminating an experiment was quite fast. The thermocouples were calibrated using a Biddle Instruments Versa-Cal Calibrator.

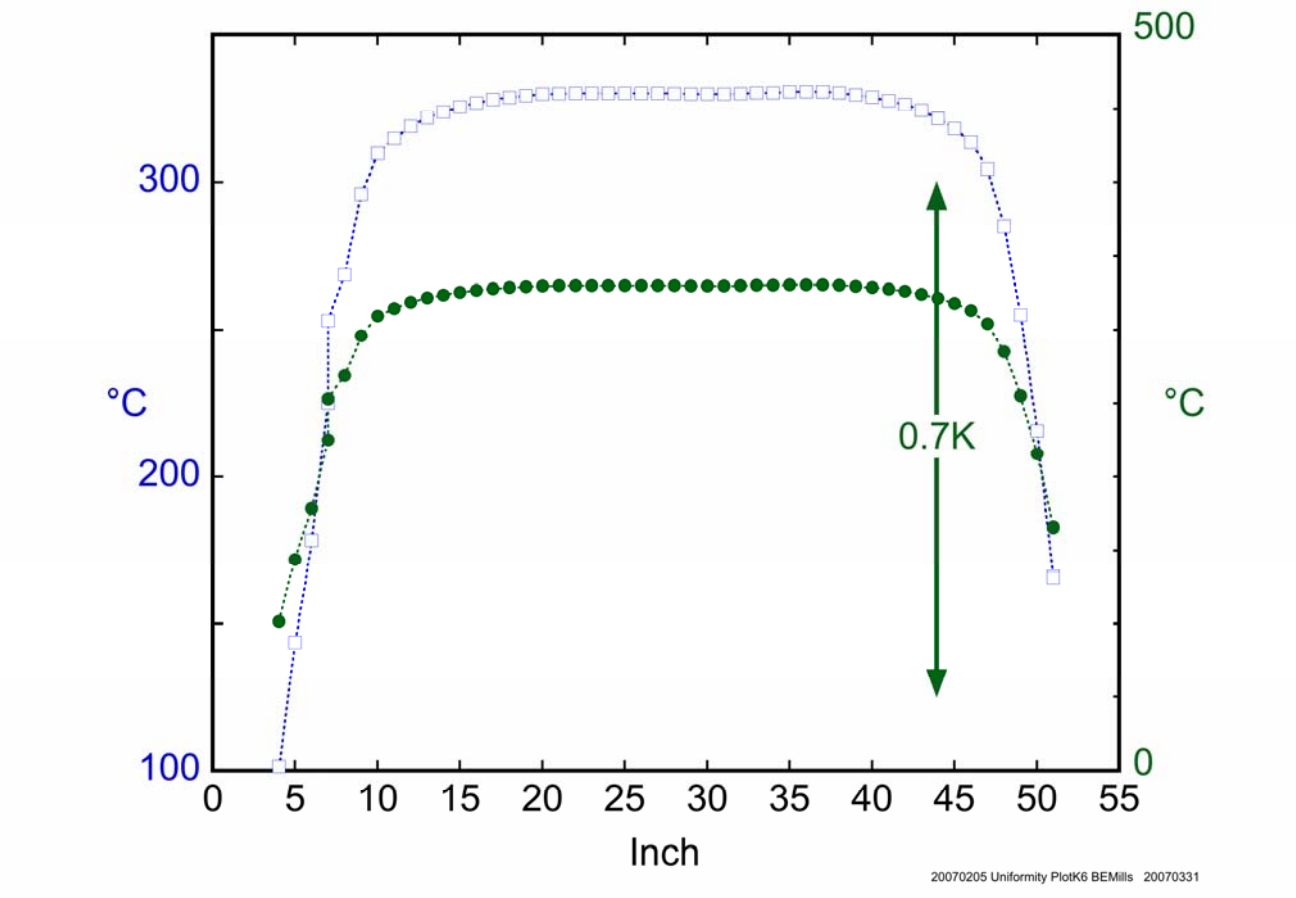

Figure 2. Temperature variation along furnace showing less than 1 K variation in a large section of tube.

Air was excluded from the samples using flowing helium. An RKI Instruments model GX-2001 battery powered oxygen monitor that was calibrated at 10% and atmospheric oxygen showed that oxygen was not detected in the furnace tube after only a short time. The partial pressure of water over the samples was maintained by passing a portion of helium through water. The line for the moist gas was heat traced until it was mixed with pure helium to generate a mixture that would not condense at room temperature. The water content of the mixed gas was measured using a General Eastern Hygro-M3 dew point monitor with a D2 sensor before being passed into the furnace. At the far end of the furnace tube a Sensirion SHT75 humidity and temperature sensor recorded the approach to equilibrium of the moisture over the samples and any change in moisture as the samples were heated. The Sensirion was operated outside of its ideal operating

range as we were using such high partial pressures of water, but it proved very sensitive, if not very accurate.

There was a concern that, as well as being at the same temperature, each sample should, to the degree possible, be exposed to the same partial pressure of water vapor. Initial experiments were started using a flow rate of 55 cc/min and 2.5 kPa water vapor pressure. An extrapolation from measurements made with Zircaloy-4 at 400°C and 1 kPa partial pressure of water indicated that the initial flow conditions chosen were expected to have a one thousand-fold excess water vapor. As further check of both the temperature and water pressure uniformity, replicate samples of one alloy (B, 1% Al) were placed at the beginning, middle, and end of each tube. These maintained their position throughout the experiment. They were chosen because they were expected to oxidize quickly and therefore be easy to measure and because there was enough material to produce the number of samples needed. For other alloys duplicates were used. Those specimens were placed either forward or back in the train of samples with respect to the flow direction and their position was rotated after each vent. One tube contained only the B samples. The 5 x 8 mm samples were not rotated, but one of each alloy was removed during each vent.

Before the experiment and after each vent the samples were each weighed at least three times on an Ohaus® Model AP2500 Analytical Plus balance, which reads to 10 μg. Unless there was evidence that the samples were gaining weight during weighing from water absorption from the air, the measurements were averaged. Samples that gained weight tended to have thick oxides so that any error caused by using only the first measurement is not significant. Samples in their containers were kept in a desiccator after they were removed from the furnace and before they were weighed.

RESULTS

Although oxygen was excluded very quickly from the outer tube and the water vapor content of the helium supplied to the tube equilibrated very fast, it was found that the moisture content of the helium as it emerged from the tube took more than a day to equilibrate. This was not due to the Sensirion humidity sensor as it has a response time of 3 sec. Even though the sensor was placed in a side passage, its effective time constant is still quite fast and cannot account for the long equilibration time. The time required to saturate the metal and glass surfaces undoubtedly causes the long equilibration time. It is important to have a good initial humidity measurement to estimate the depletion of moisture by reaction with the samples. Too high depletion will starve down-steam samples. The record of humidity during the first 45 hours of furnace operation with samples is shown in Figure 3. It was clear that there was an unacceptable level of

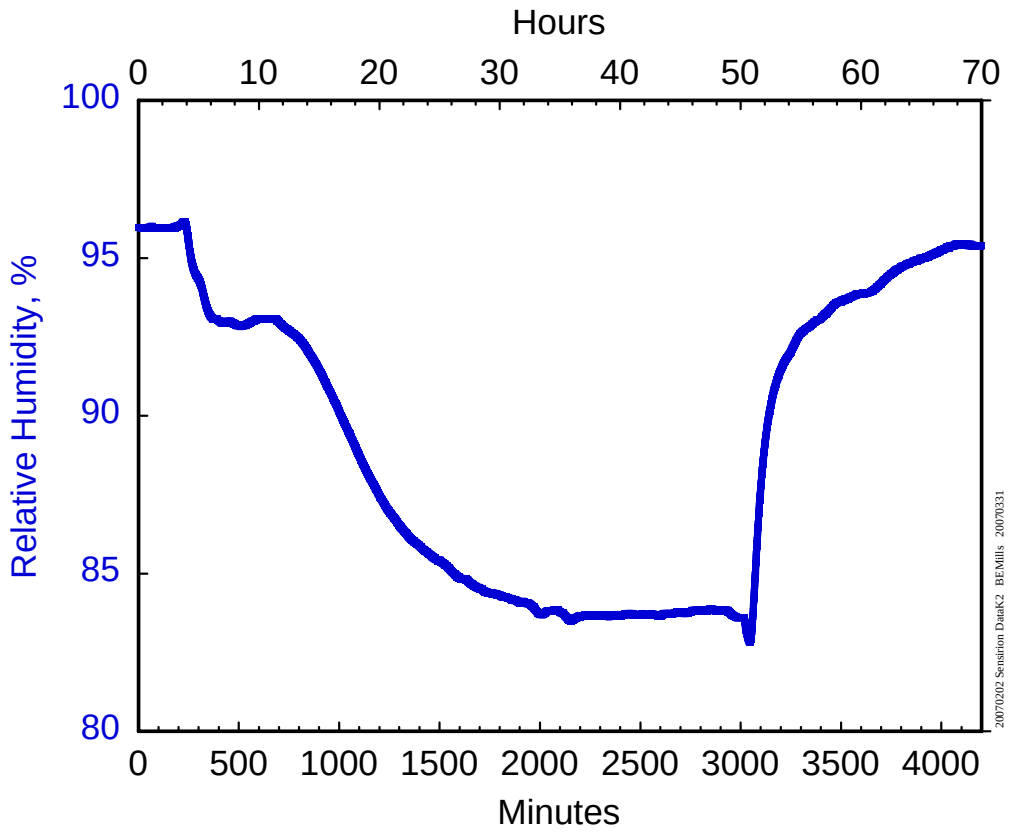

Figure 3. Decrease in relative humidity measurement of the effluent gas from the tube furnace for the first 45 hours of operation indicates some samples are starved of water vapor.

samples H, K, and M. This noticeable difference in mass does not seem too consistent with the very weak $P^{1/6}$ pressure dependence for oxidation in the literature as summarized in a recent

review article [Causey]. Subsequent exposures were done at five times the flow rate and this effect was no longer observed.

The weight gain of the samples after 45 hours at 300°C is shown in Figure 4.

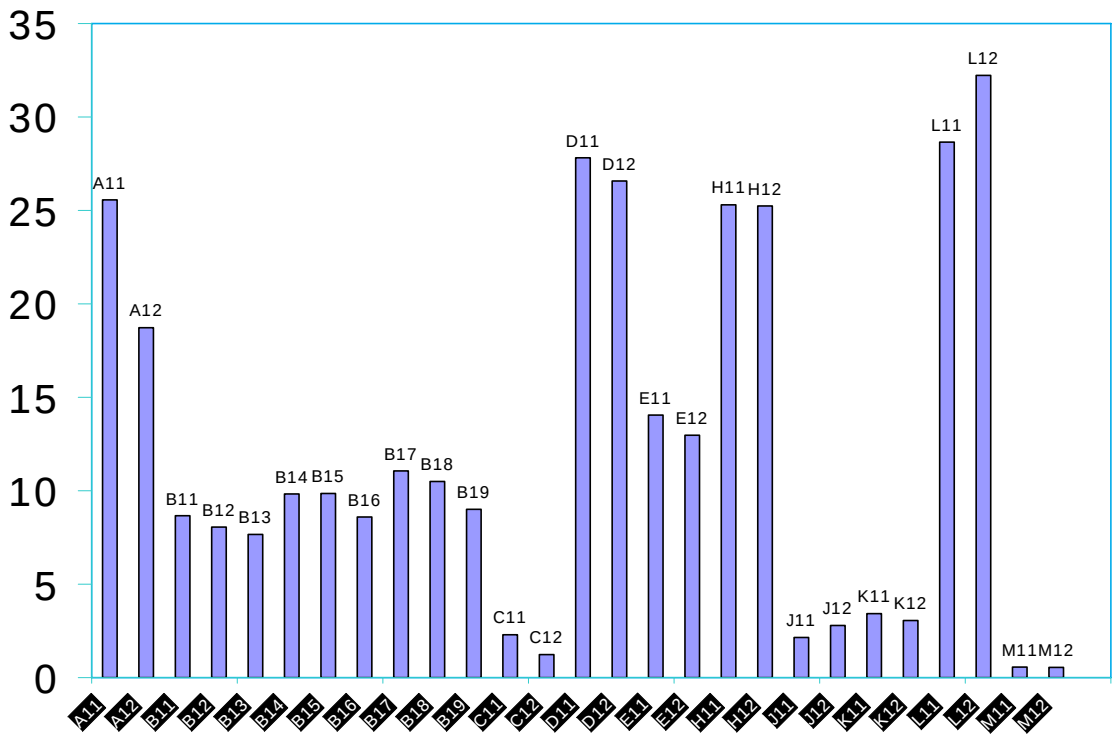

Figure 4. Mass gains of the samples after 45 hours at 300°C and 2.5 kPa water vapor partial pressure**.**

A map of the relative sample positions is shown in Figure 5. Samples B11, B14, and B17 are at the entrance of the flow. B12, B15, and B19 at the end of the flow and the other Bs are in the middle. Samples A11, C11, D11, and E11 and samples H12, J12, K12, L12, and M12 are earlier in the sample train than their duplicates. The effect of water depletion is clearly evident in all but samples H, K, and M. This noticeable difference in mass does not seem too consistent with the very weak $P^{1/6}$ pressure dependence for oxidation in the literature as summarized in a recent review article [Causey]. Subsequent exposures were done at five times the flow rate and this effect was no longer observed.

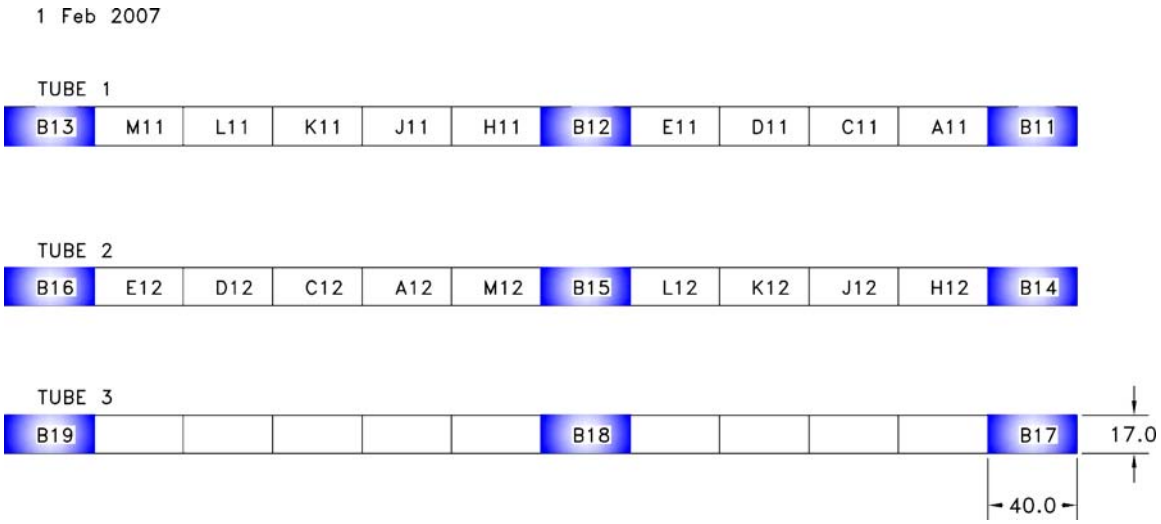

Figure 5. Initial relative position of sample in quartz furnace tubes. B samples remained in the same position; others were rotated, varying the tube number and the relative position.

Zirconium-aluminum alloys are reported to oxidize in water and steam immediately to form a friable spalling white oxide film. Complete destruction was observed for a 0.25% Al alloy at 325°C [Parfenov]. This work did not observe such catastrophic effects at this lower partial pressure and temperature.

Weight gain over the course of 35 days for the B samples (Zr 1% Al) shows very little variation and no systematic variation with position (Figure 6). Estimated oxide thickness is based on all of the weight gain producing zirconium oxide with a density of 5.89 g/cc. The edges are not included in the calculation because they are very small and they were Electro Discharge Machined (EDMed), which renders the surface composition atypical. As noted above, copper surface contamination can accelerate oxidation in the initial stages. The oxide becomes somewhat protective after about two weeks as seen by the decrease in oxidation rate.

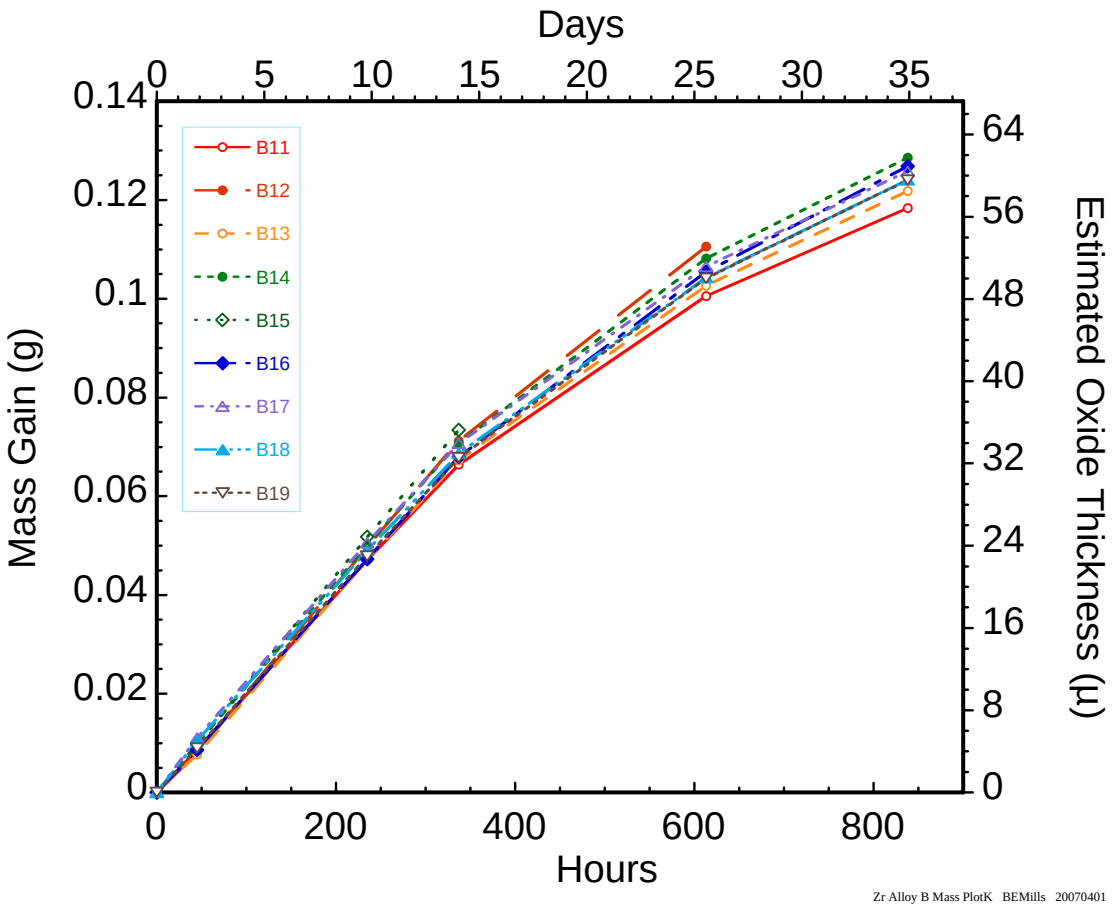

Figure 6. Oxidation of Zr 1% Al alloy.

By comparison samples E, which have 0.5% Ni in addition to the 1% Al, show an initially higher oxidation rate, followed by a greater decrease in rate (Figure 7).

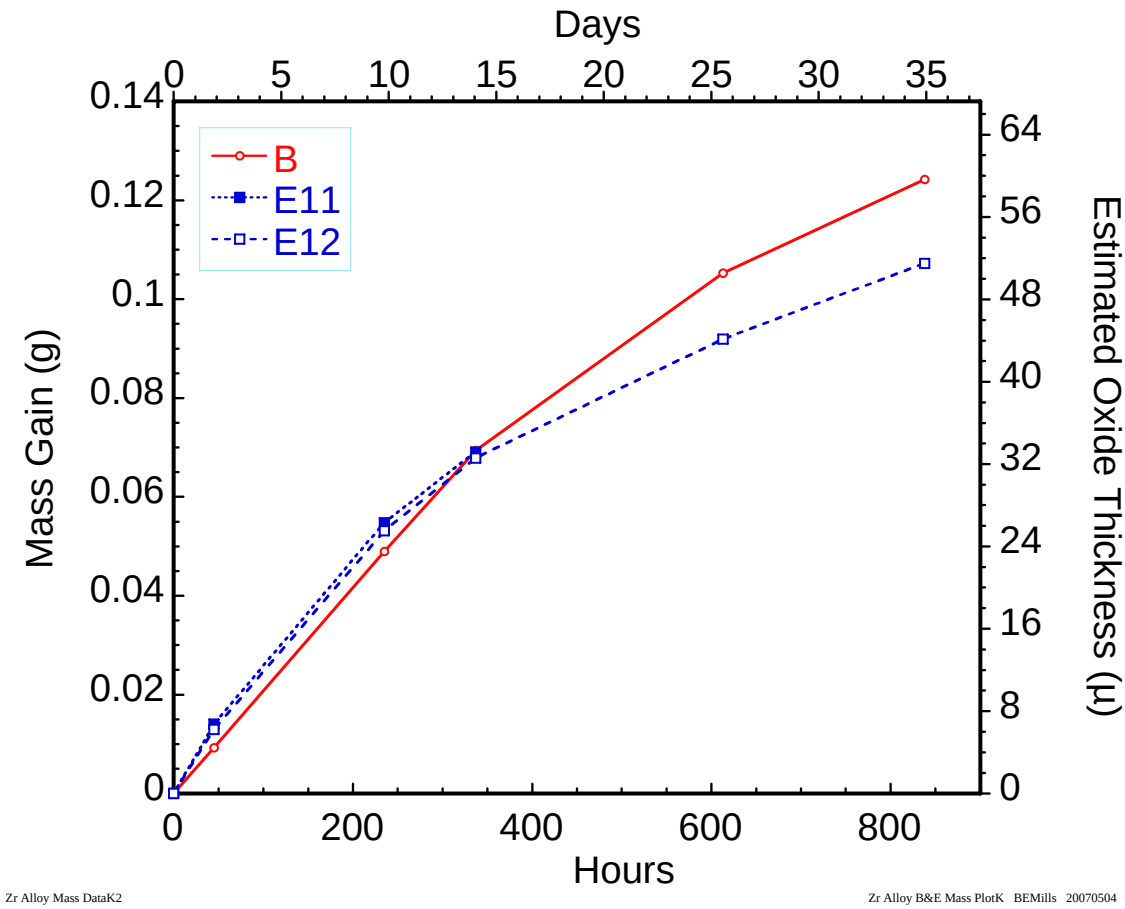

Figure 7. Addition of 0.5% Ni to the 1% Al alloy produces an oxide that becomes more protective with time. B alloys are represented by their average mass gain.

The effect of addition of 1.5% Y and of 1.5% Y, 0.5% Ni is shown in Figure 8. These alloys do not show significant protective oxide growth and, again, Ni decreases the oxidation rate over the 35 day time period.

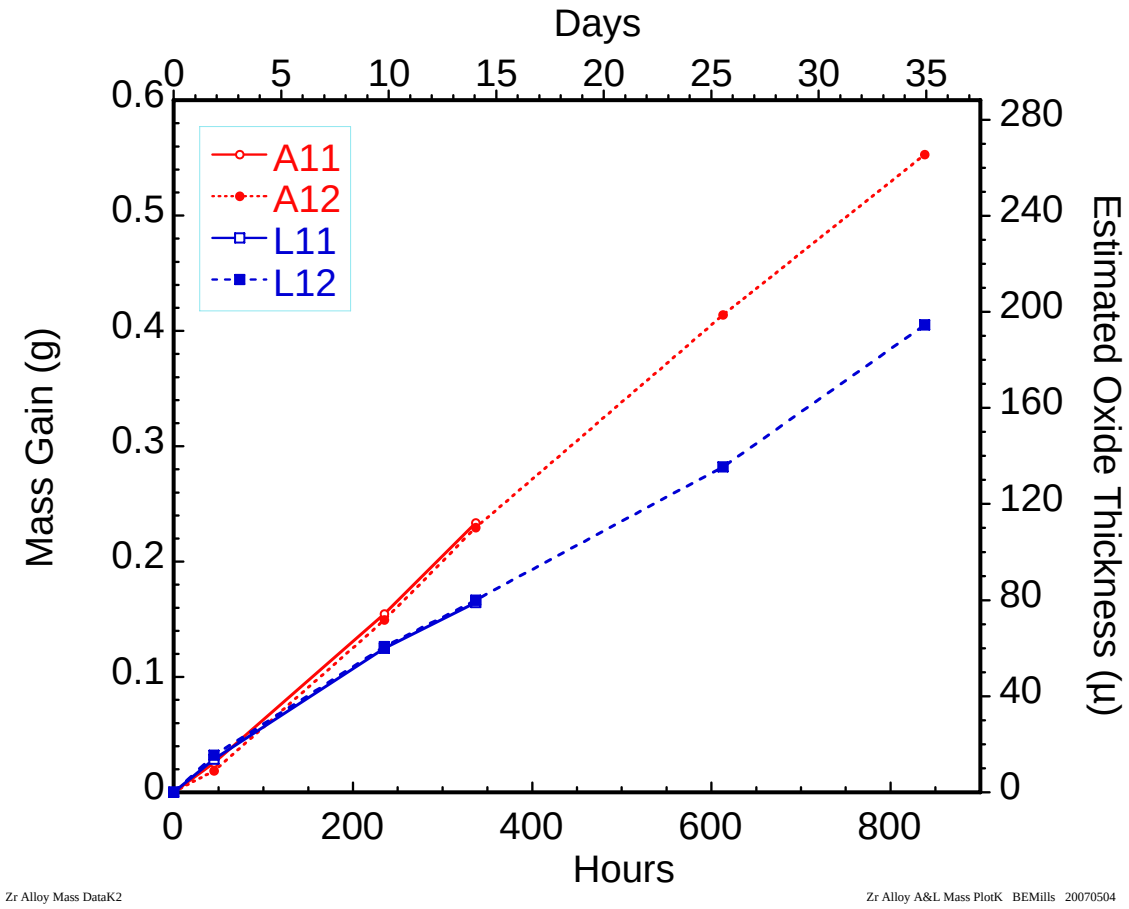

Figure 8. Comparison of oxidation rate for 1.5% Y alloys without (A) and with (L) the addition of 0.5% Ni shows that Ni inhibits oxide formation.

Vanadium is thought to increase corrosion resistance at low concentration but to decrease corrosion resistance at concentrations above 2-3% [Parfenov].

Three alloy compositions were made with the addition of 5% V. One had only V and two had additional Ni at the 0.1 and 0.7% level (Figure 9). In this case the oxide is not noticeably protective and the addition of Ni increases the oxidation rate. This also is the first example shown where the duplicate samples do not oxidize identically.

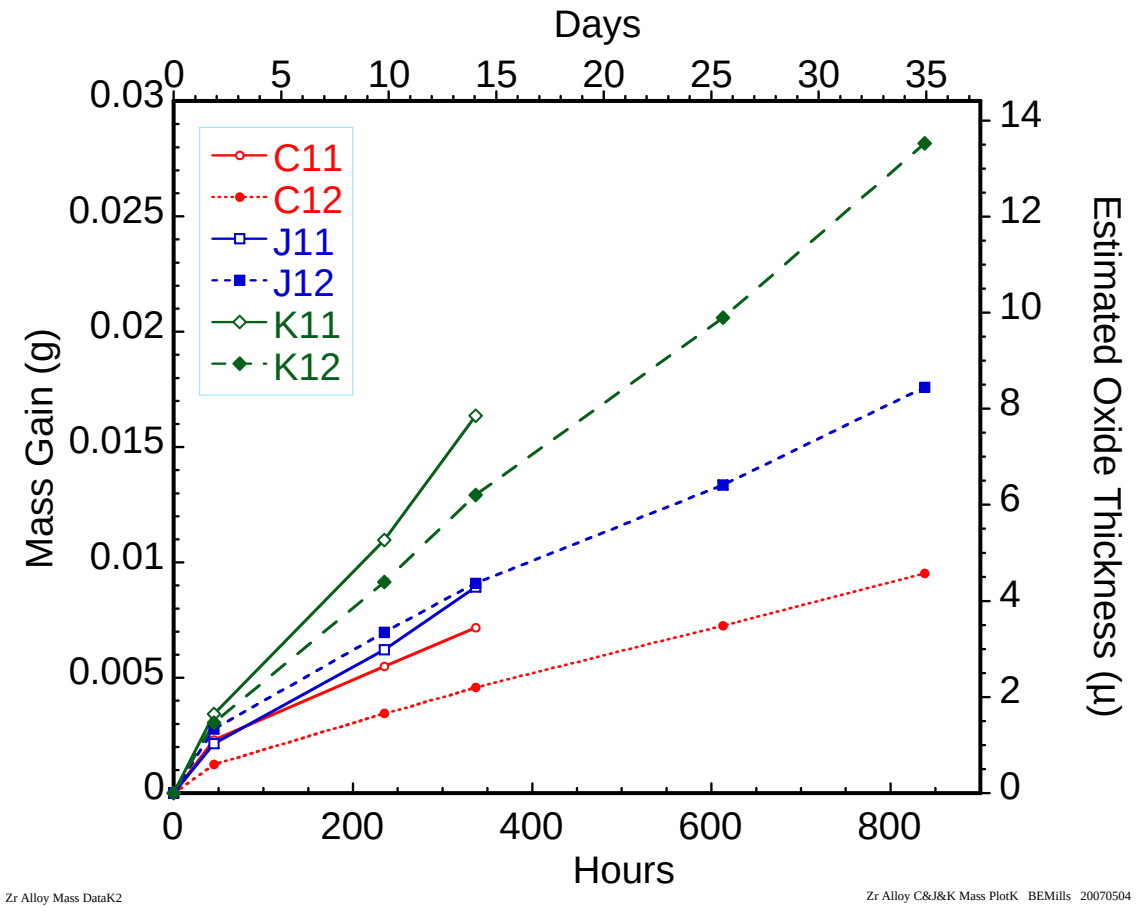

Figure 9. Oxidation of 5% V alloys C, J, and K with 0, 0.1, and 0.7 % Ni additions.

This can be understood by observing the difference in surface morphology of each of the samples (Figure 10). The C and J alloys, with 0 and 0.1 % Ni, have a visibly distinct non-uniform surface texture, which could lead to non-uniformity in oxidation. The 0.7 % Ni alloy K does not show the same surface texture variation, but K11 has much more visible surface flaws than K12 as well as a higher oxidation rate. Surface preparation has been shown to affect the corrosion rate in zirconium alloys with rough abraded surfaces more than 4 times as reactive as sputtered or electropolished surfaces. Diamond polished and pickled surfaces are intermediate in reactivity [Wanklyn].

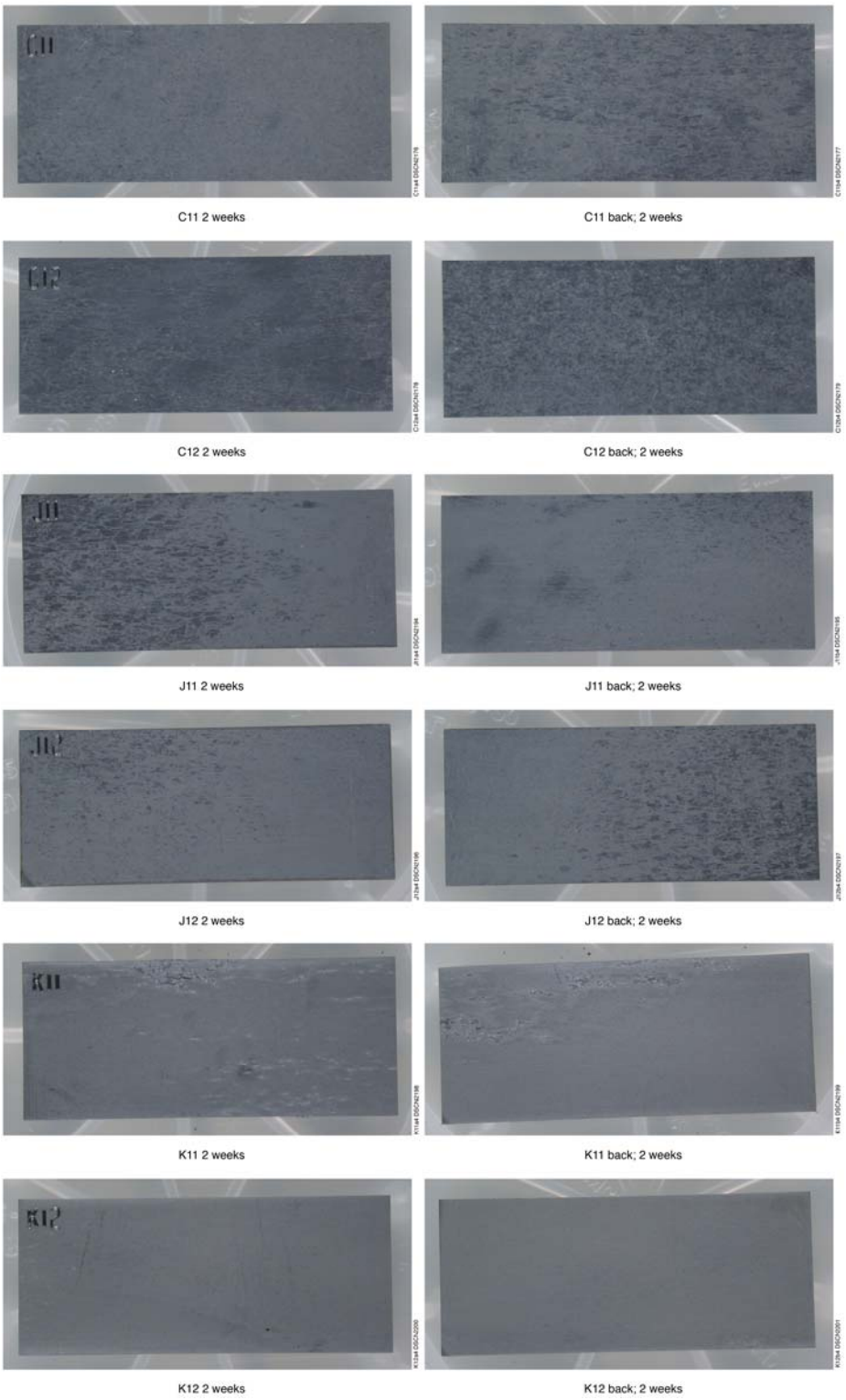

Figure 10. Surface appearance of 4x17 mm 5% V alloys C, J, and K with 0.0, 0.1, and 0.7 % Ni additions respectively after two weeks.

Titanium was the principle alloying addition in three sets of samples (Figure 11). Alloy D contains 1 % Ti. Interestingly it oxidizes more readily than Alloys H and T, which have twice as much Ti. Alloy D looses its oxide in large neat flakes that are easy to collect as seen in Figure 12. At the two week point D11 had not yet flaked, though observing the edges it appears that the oxide was beginning to loose its adherence and it had flaked by the next vent. D12, on the other hand, had completely flaked. It was possible to collect almost all of the flakes for weighing. Both alloys H and T have 2% Ti and 0.5 % Ni.

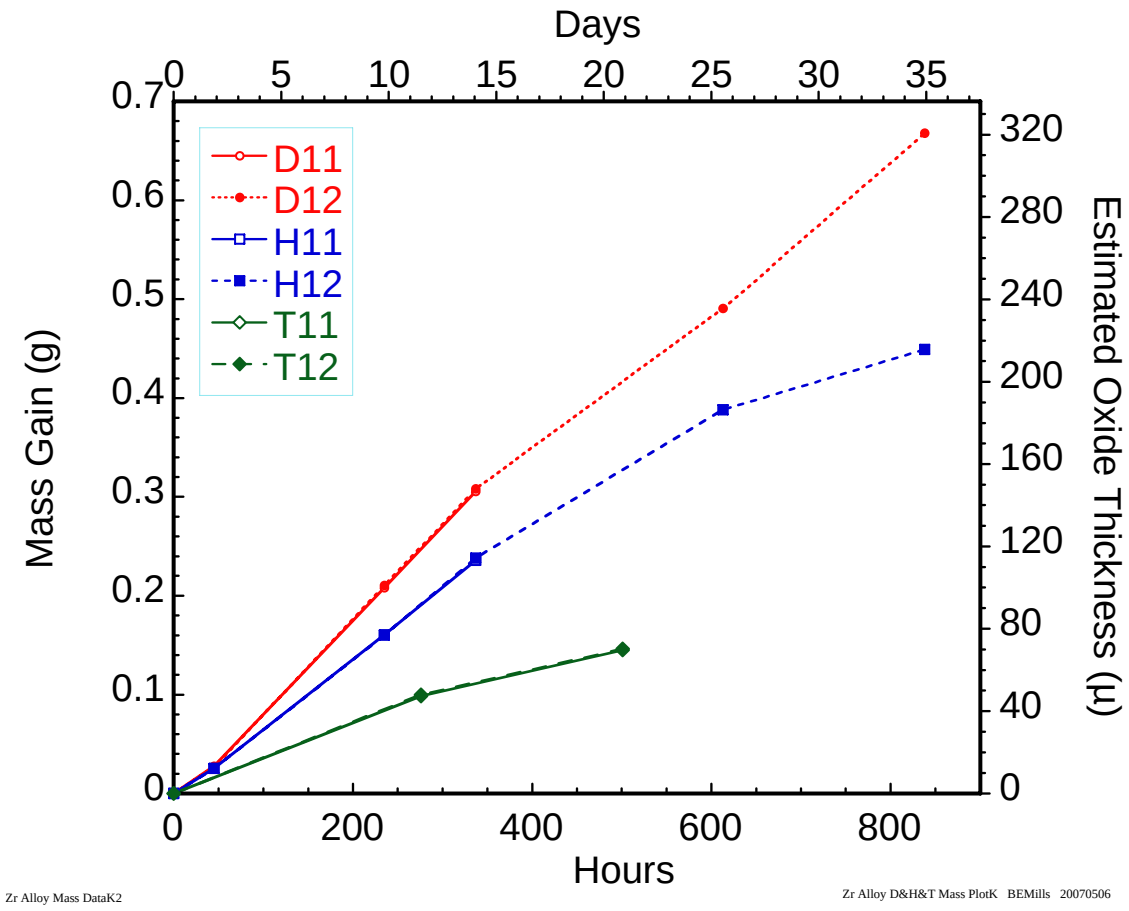

Figure 11. Oxidation of Zr-Ti alloys. Alloy D contains 1% Ti; Alloys H and T both have 2%Ti and 0.5% Ni. Alloy T was hot rolled at a lower temperature to reduce pitting during rolling.

The latter was hot rolled at lower temperature to preclude pitting or surface stringers seen in the photos of Alloy H in Figure 12. This was effective as seen in the lower photos in Figure 12. The smoother material of Alloy T oxidizes more slowly than the rougher material of Alloy H. This is consistent with short term (up to 6 hours) experiments where Zr samples abraded to produce a higher surface area oxidized more than twice as fast as chemically polished samples in dry oxygen at the lowest temperature reported (450°C) [Gulbransen, 1957].

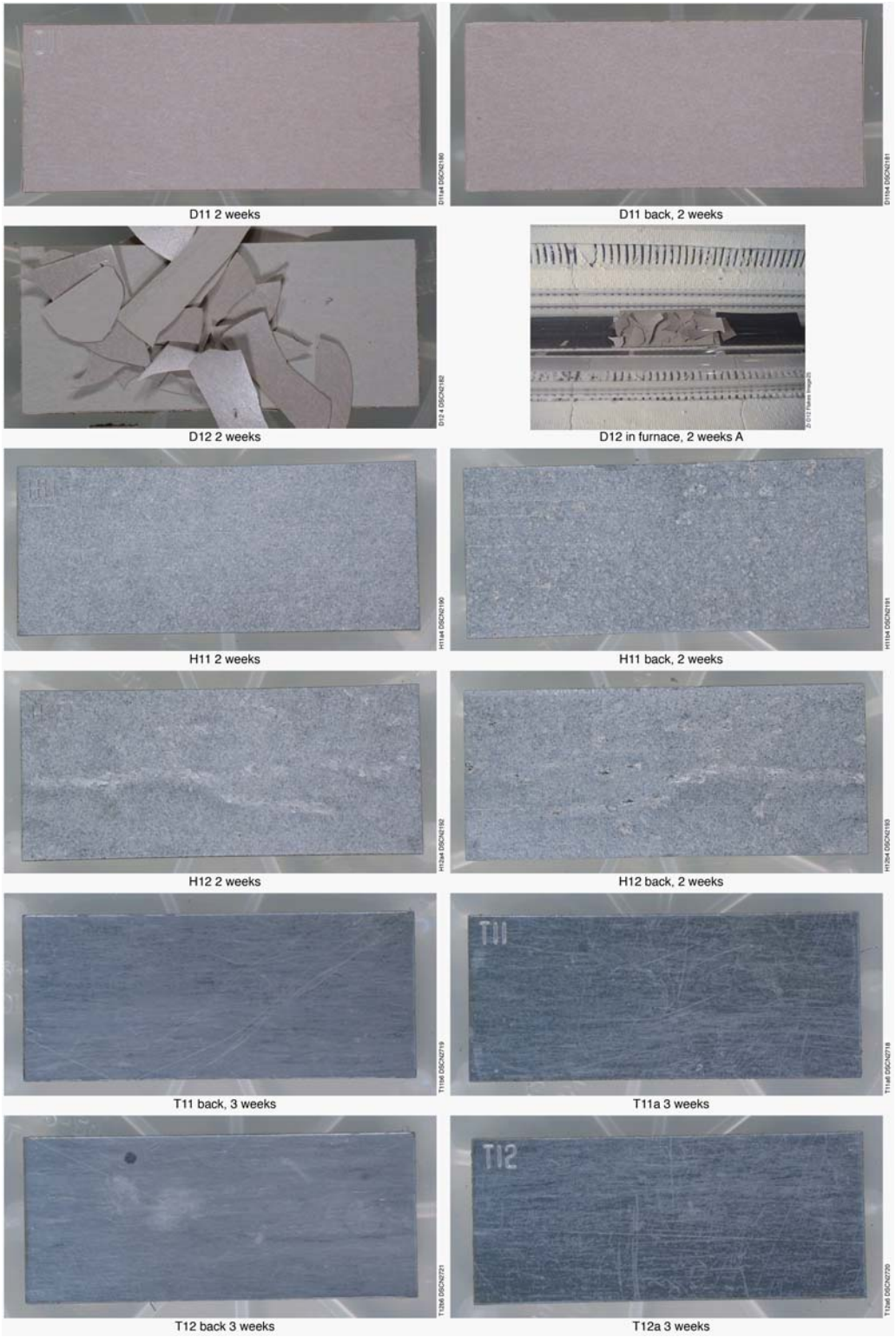

Figure 12. Surface appearance of 4x17 mm coupons of Alloy D (1% Ti) and Alloys H and T (2% Ti, 0.5% Ni). D is shown with its oxide both out of and in the quartz tube in the open furnace. The oxide has flaked off in very coherent sheets that, although some have "landed" on neighboring samples, were easy to retrieve and weigh.

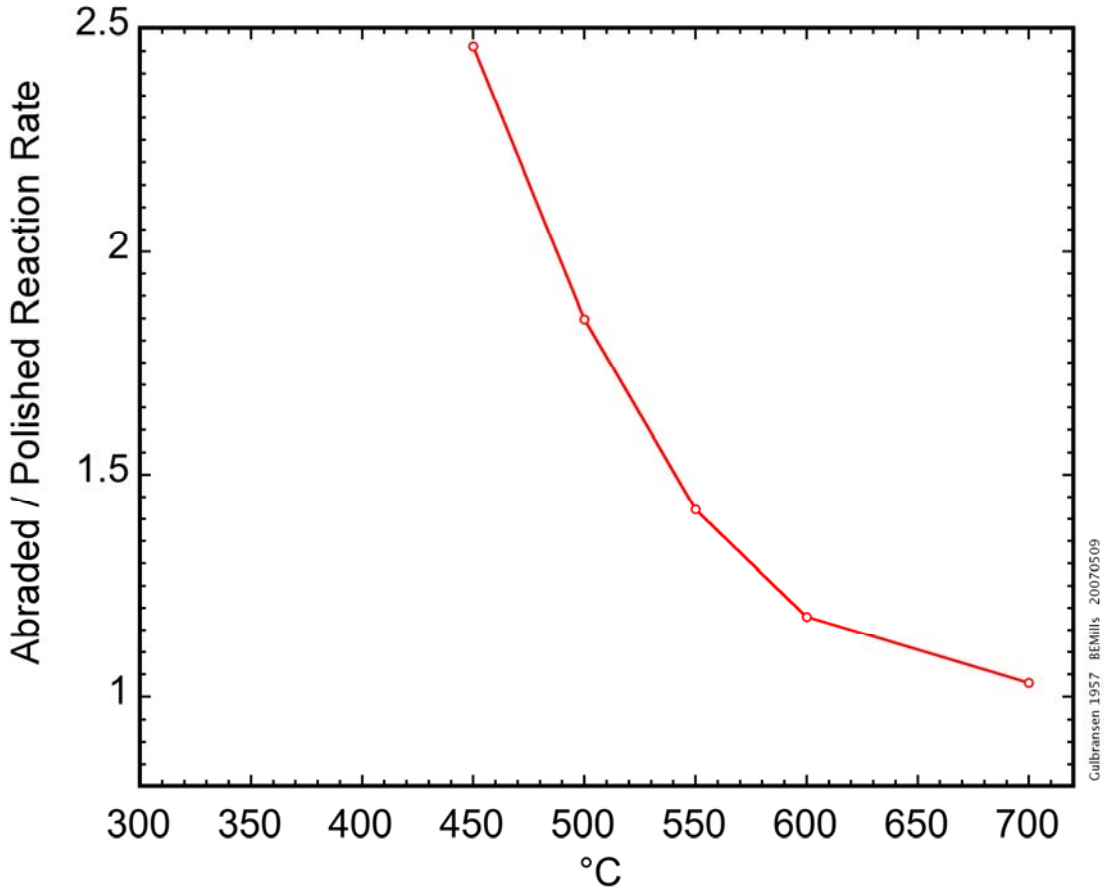

Figure 13. Relative reaction rate of abraded and polished Zr in dry oxygen at various temperatures (Gulbransen, 1957).

If the data are extrapolated to lower temperature, we might expect a more pronounced effect of roughness at 300°C (Figure 13). The decrease in corrosion rate observed with the addition of Ni is qualitatively consistent with the Misch work sited by Parfenov that 0.1% Ni in a 0.5% Ti alloy decreased the corrosion rate 53% at 350°C in water.

Two alloys were made with Sc additions: a 0.1 % Sc Alloy S and a 0.5 % Sc, 0.1 % Ni Alloy V. Their oxidation rates are shown in Figure 14. The high Sc plus Ni alloy is 28 times as reactive as the low Sc, no Ni alloy, suggesting that the addition of Ni may enhance oxidation in this case. Since alloys of the same Sc composition with different Ni compositions were not tested, this has not been confirmed.

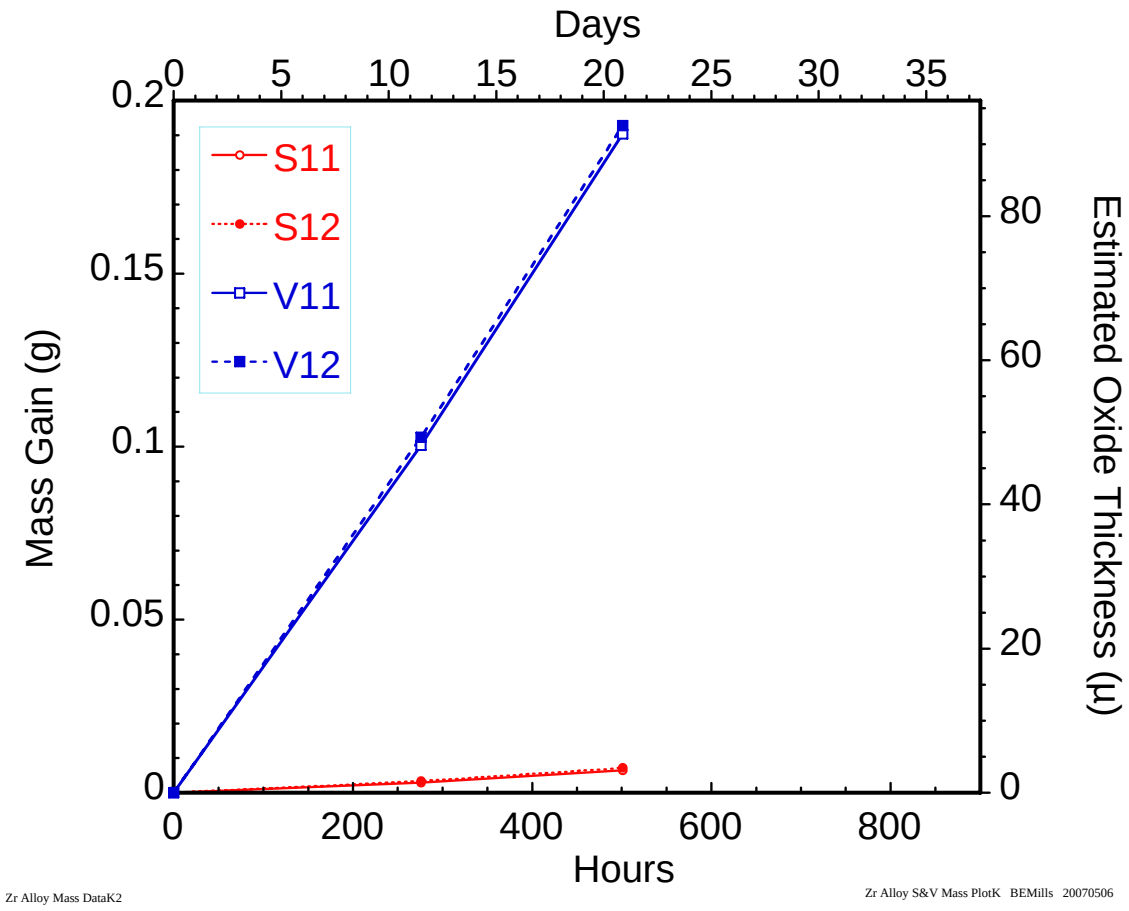

Figure 14. Oxidation of Scandium alloys. Alloy S contains 0.1 % Sc; Alloy V is 0.5 % Sc, 0.1 % Ni. Although the samples were oxidized for a shorter time, the time scale shown is the same as for previous plots.

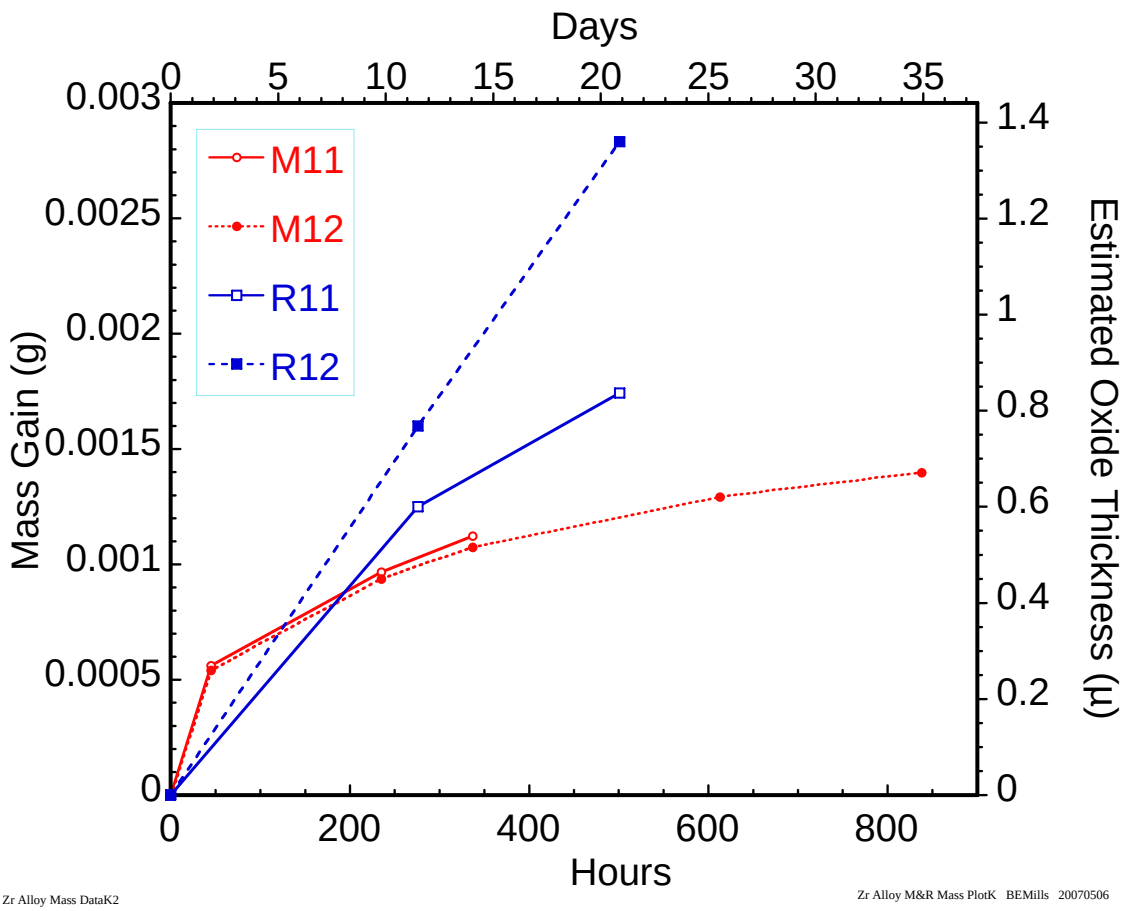

Figure 15. Oxidation of Zr-2 (Alloy M) and Zr, 280 ppm N (Alloy R).

Shown in Figure 15 is the oxidation of the commercial alloy Zircaloy-2 (Zr-2, M in figures), which is specified as zirconium with 1.20-1.70% tin, 0.07-0.20% iron, 0.05-0.15% chromium, and 0.03-0.08% nickel. Also shown is the oxidation of Zr with 280 ppm nitrogen. Nitrogen was chosen because of the evidence that nitrogen content above 40 ppm degrades the corrosion resistance [Craig]. The protective behavior seen in the Zr-2 (Alloy M) results is the closest seen to the literature summarized in [Causey] where oxidation is seen to be initially parabolic, then cubic, and finally linear. With Zr-2 the oxide has not reached the 2-3μ thickness necessary for transition to linear corrosion.

DISCUSSION

Figure 16 summarizes the mass gain results from all the alloys. Two plots with very different mass scales are necessary to visualize the data because of the large dynamic range of the reaction rates. The right hand scale is calculated based on zirconium oxide as the only corrosion product. Each alloy is represented by the average of the two or nine samples that were used in the experiment. Some do not go to the full time because they were introduced in the middle of the experiment. If the replicates did not behave identically, there is a step in the slope of the data when one of the replicates was removed from test.

The 1% Ti alloy (D) oxidizes the fastest, producing a linear mass gain curve with the duplicate samples behaving identically. This alloy is the only one that lost large amounts of oxide to flaking. Addition of 2% Ti and 0.5% Ni (alloy H) leads to a material that oxidizes at a lower rate than with the lower Ti concentration and no Ni. Alloy T, at nominally the same composition as alloy H, shows a markedly lower oxidation rate, indicating that processing conditions matter even though Ti and Zr are fully miscible. Perhaps an impurity level introduced during the higher temperature rolling led to the poorer corrosion behavior of alloy H. Duplicate samples behaved identically. This leads us to notice the slight decrease in reactivity of alloy T from about 11 to 21 days and the corresponding decrease for alloy H, which might otherwise have been attributed to the attrition which is expected as the oxide grows thicker and has its edges knocked off. The reactivity of these Ti Ni alloys may be decreasing slightly with oxide thickness.

Almost at reactive as the titanium alloys are the yttrium alloys, although the concentration of Y in alloy A was 1.5%. The 1.35% Y 0.5% Ni alloy L oxidizes more quickly initially than alloy A, but ultimately reacts more slowly as the oxidation progresses. The duplicate samples behaved identically after the initial few hours when the down-stream samples were water-starved. Even then, each of the L samples oxidized more quickly than any of the A samples.

Less reactive than either Y sample are the scandium samples. At 0.09% Sc, alloy S is not easily comparable with alloy V at 0.45% Sc and 0.1% Ni and 28 times the reactivity. These alloys were only exposed to elevated temperature and water vapor pressure for about 21 days. The limited number of data points suggests that alloy S may have had a parabolic or cubic initial reaction rate followed by a transition to a linear rate after the first data point was taken at about 11 days and 1.5μ oxide thickness. The high Sc Ni alloy reaction rate appears linear throughout.

The 1% aluminum alloys, which are both less reactive than the high Sc Ni alloy, display non-linear kinetics to quite large oxide thicknesses. After an initially higher reaction rate for the 0.5% Ni alloy E, alloy B, with no additional Ni, overtakes the net oxidation of alloy E. This takes place after about 13 days and at an oxide thickness of about 32μ. Duplicates, or in the case of alloy B 9 identical samples, show similar behavior.

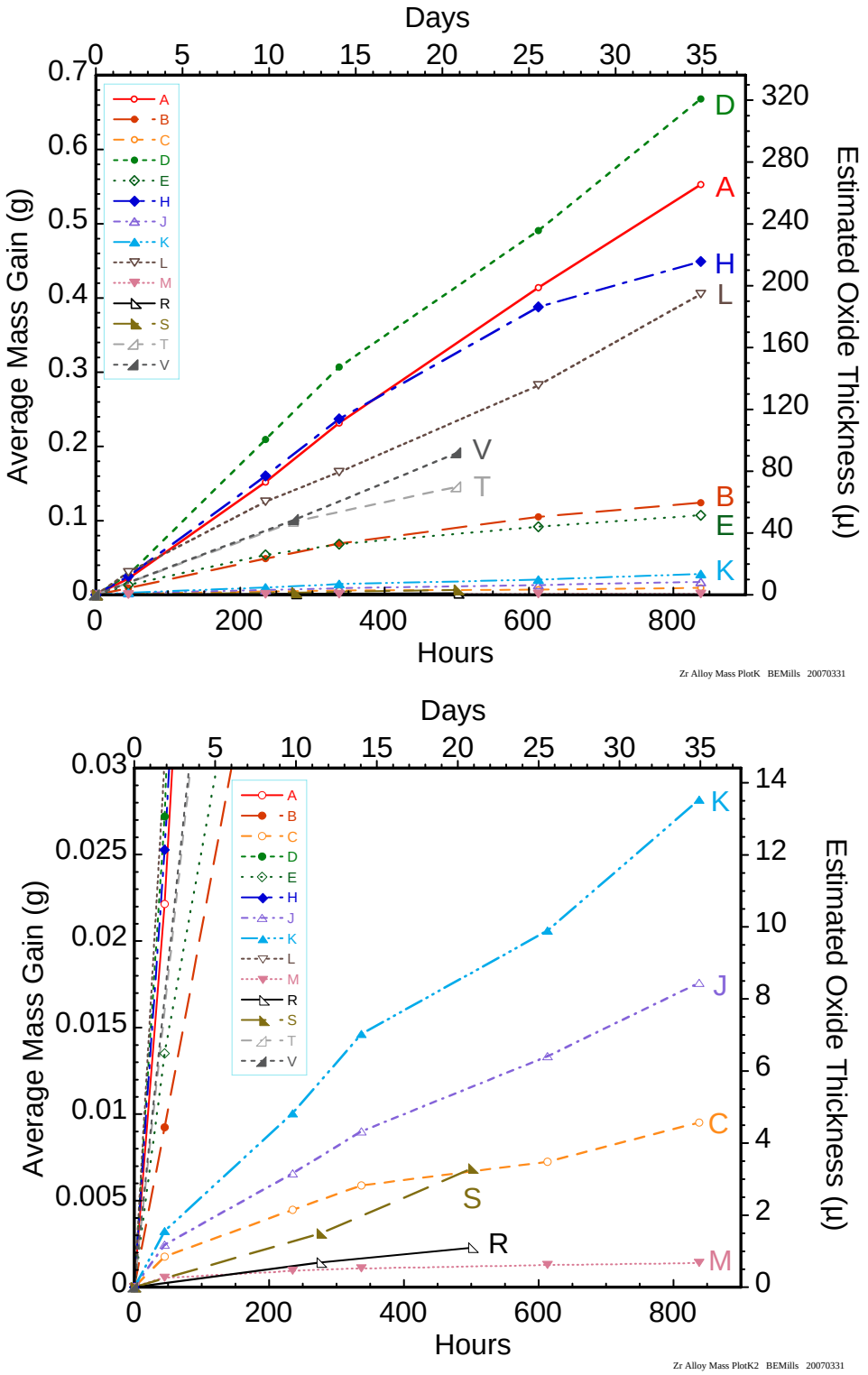

Figure 16. Mass gain and calculated oxide thickness averaged for duplicates or multiples of each alloy tested. Note the difference of mass scale. Compositions listed in Table I.

The Vanadium alloys are the only example with essentially identical principle alloying addition (4.7-4.83% V) with three different nickel concentrations. Alloy C has no Ni; alloy J, 0.1%; alloy K, 0.65%. In each case the Ni increases the reactivity of the alloy, although 0.65% Ni has only about twice the effect of 0.1% Ni. Although the order of reactivity holds up for all the samples of each alloy, the duplicate samples do not behave identically. This is probably due to localized differences in composition or microstructure as evidenced by the differences in texture seen on the surfaces of the samples of alloys C and J and the surface flaws seen in the alloy K samples.

The one sample that had 280 ppm nitrogen added is alloy R. The duplicate samples did not behave identically, with a final oxide thickness about 60% thicker on one sample than the other. This degree of difference is hard to attribute to the pitting on the samples, which, although prominent, does not take up much area and seems to be present on all of the samples. Only two sets of measurements were made on these samples and none were taken at short times. By the first measurement, alloy R mass gain had overtaken the mass gain for alloy M, the Zircaloy-2 samples.

The Zircaloy-2 (alloy M) duplicates behaved identically, showing the expected protective kinetics. During the initial two day period when they did not have identical partial pressures of water above them, they put on the largest mass per day and still behaved identically. This is consistent with the expected exp (1/6) dependence on pressure [Causey]. This experiment was not long enough to break through to the linear kinetics expected with thicker oxides.

CONCLUSIONS

All of the experimental alloys tested corrode faster than Zircaloy-2; some at a rate almost 500 times faster in up to 35 days.

Although some of the alloys show a decreasing reactivity with oxide thickness, this effect is in none as prominent as it is for the commercial Zircaloy-2. However, the effect persists to thicknesses much greater that the 2-3μ reported to be the transition point for an increase to fast linear kinetics for commercial alloys. This effect is most prominent in the aluminum alloys but may also be seen in the titanium alloys.

Some of the duplicate alloy coupons behaved identically and some did not. This indicates whether or not uniform samples were made. The aluminum, yttrium, titanium, scandium, and Zircaloy-2 coupons behaved identically. The vanadium and nitrogen alloys did not. In some cases these differences coincided with observed differences in surface texture or finish. In other cases differences in surface features were not reflected in differences in duplicate behavior. Identical 2% Ti 0.5% Ni heats were rolled at different temperatures and the result was a factor of two differences in the reactivity.

Nickel additions to binary zirconium alloys cause an initial increase in reaction rate. This is seen in aluminum, yttrium, and vanadium alloys. Although the alloys are not completely comparable, this may also apply to titanium and scandium alloys as well. As the oxide thickness increases, the oxidation rate decreases with increasing Ni addition until, at a thickness of about 30μ, the net oxidation of the Ni alloy becomes less than that of the 0% Ni alloy. The only case where there are three different Ni concentrations is with the 5% V alloy. In this case the final oxide thicknesses were below 14μ and no cross-over to lower reaction rate with higher Ni concentration was seen. These alloys do, however, permit us to compare the effectiveness of the amount of the nickel added. 0.65% Ni addition is about twice as effective 0.1% Ni in increasing oxidation rate.

Nickel addition, in increasing the initial reactivity and decreasing the final reactivity, seems to give us the property we desire in a liner material. If Ni could be added to Zircaloy-2 it may be ideal.

REFERENCES

Causey, R. A., D. F. Cowgill, and R. H. Nilson, 2005, *Review of the Oxidation Rate of Zirconium Alloys*, SAND2005-6006. Sandia National Laboratories, Livermore, CA.

Cox B. 1976, Oxidation of Zirconium and its Alloys, in *Advances in Corrosion Science and Technology*, vol. 5, M. G. Fontana and R. W. Staehle, ed., pp. 173-391.

Craig, B. D., ed., 1989, *Handbook of Corrosion Data*. ASM International, Metals Park, OH.

Denton, R. J. 2002, from Tritium Producing Burnalde Asorber Rod (TPBAR),

Douglass, D. L., 1971, *The Metallurgy of Zirconium, Supplement 1971*. International Atomic Energy Agency, Vienna.

Johnson, A. B., Jr., E. R. Gilbert, and R. E. Williford, 2006, *Tritium Technology Program Selection of Candidate Zirconium Alloys for ATR Test*, TTP-1-2181, Pacific Northwest National Laboratories, Hanford, WA.

Kass, S., 1964, The Development of the Zircaloys, in *Corrosion of Zirconium Alloys*. ASTM Special Technical Publication No. 368, pp. 3-27, American Society for Testing and Materials, 1916 Race St., Philadelphia, PA.

Knittel, D. R., 1983, Zirconium, in *Corrosion and Corrosion Protection Handbook*, P. A. Schweitzer, ed., pp. 191-219, Marcel Dekker, New York.

Nasrallah, M. M., and D. L. Douglass, 1975, The Oxidation Behavior of Zr-0.5Y Alloy, in *Oxidation of Metals*, vol. 9, pp. 357-365.

Parfenov, B. G., V. V. Gerasimov, and G. I. Venediktova, 1967, *Corrosion of Zirconium and Zirconium Alloys*. Israel Program for Scientific Translations, Jerusalem, 1969, translation.

Schemel, J. H., 1977, *ASTM Manual on Zirconium and Hafnium*. ASTM Special Technical Publication No. 639, American Society for Testing and Materials, 1916 Race St., Philadelphia, PA.

Thomas, D. E., 1955, Corrosion in Water and Steam (Corrosion of Zirconium and its Alloys), in *The Metallurgy of Zirconium*, B. Lustman and F. Kerze, Jr., ed., pp. 608-686. McGraw-Hill, New York.

Wanklyn, J. N., 1964, The Development of the Zircaloys, in *Corrosion of Zirconium Alloys*. ASTM Special Technical Publication No. 368, pp. 58-75, American Society for Testing and Materials, 1916 Race St., Philadelphia, PA.

Yau, T., 1989, Zirconium, in *Corrosion and Corrosion Protection Handbook*, P. A. Schweitzer, ed., pp. 231-281, Marcel Dekker, New York.

Yau, T. and R. C. Sutherlin, 2005, Corrosion of Zirconium and Zirconium Alloys, in *ASM Handbook*, vol. 13B. ASM International, Materials Park, OH.

DISTRIBUTION:

Pacific Northwest National Laboratory
902 Battelle Boulevard
Richland, WA 99352
Attn: Cheryl K. Thornhill, Project Director (5)
Glenn Hollenberg (1)
David Senor (1)

Office of Stockpile Technology and Special Materials
U. S. Department of Energy
Albuquerque Operations Office
P. O. Box 5400
Albuquerque, NM 87185-5400
Attn: Nanette D. Founds, NA-123 (Phone: 505-845-4212) (1)

1	MS9001	P. J. Hommert, 8000; Attn:
	MS9001	C. A. Nilsen, 8000
	MS9002	L. A. Houston (A), 8500
	MS9004	J. M. Hruby, 8100
	MS9054	T. A. Michalske, 8300
	MS9151	L. M. Napolitano, MS8900
	MS9153	C. L. Knapp, 8200
1	MS9042	D. M. Kwon, 8770
1	MS9042	M. L. Chiesa, 8774
1	MS9161	A. E. Pontau, 8750
1	MS9161	D. F. Cowgill, 8758
1	MS9161	R. H. Nilson, 8755
1	MS9161	S. W. Allendorf, 8756
1	MS9291	B. A. Simmons, 8755
1	MS9402	J. E. Goldsmith, 8772
1	MS9402	J. A. Whaley, 8758
5	MS9403	B. E. Mills, 8778
1	MS9403	R. A. Causey, 8758
1	MS9403	T. J. Shepodd, 8778
1	MS9404	E-P. Chen, 8776
1	MS9405	R. W. Carling, 8700
1	MS9409	A. Ting, 8757
1	MS9409	C. D. Moen, 8757
2	MS9018	Central Technical Files, 8945-1
2	MS0899	Technical Library, 4536

This page intentionally left blank.